

# High-strength (5 GPa) steel wire: an atom-probe study

H.K.D.H. Bhadeshia and H. Harada

Department of Materials Science and Metallurgy, University of Cambridge /JRDC, Pembroke Street, Cambridge CB2 3QZ, UK

Received 10 August 1992; accepted for publication 4 September 1992

The strongest commercial fibre, "Scifer" is investigated with a view to explaining its strength and discovering its structure at very high resolution. It is found that the ultra-high-strength steel fibre owes most of its strength to the very fine dislocation cell structure which originates during the very severe deformation imparted in the course of fibre manufacture. In addition, the carbon in the alloy is to a large extent forced into solid solution by a process akin to mechanical alloying, and this adds significantly to the overall strength.

## 1. Introduction

The ideal slip resistance of a metal is about  $G/30$ , where  $G$  is the elastic modulus in shear. It is well established that this incredible level of strength can be achieved as the crystal becomes smaller in size [1]. In fact, crystals in the form of whiskers can be so strong (about 14 GPa) that elastic strains of the order of a few percent can easily be achieved, with nonlinear elastic phenomena manifesting at the larger strains. However, the strength of whiskers tends to be very sensitive to size (fig. 1), and the whiskers are very difficult to manufacture. It is for this reason that the highest strength steel wire has for many decades been piano wire which consists of heavily drawn fine pearlite with a tensile strength of about 3 GPa.

A remarkable increase in strength (from 3 → 5 GPa) has recently been achieved for steel wire with a microstructure entirely different from that of pearlite [2]. The wire, which is made by drawing, has the trade name *Scifer* and is currently the strongest available continuous fibre by some 2 GPa. The purpose of the present work was to investigate the origins of the strength of *Scifer*. The atomic resolution technique of field ion microscopy (FIM) is an ideal tool for studying *Scifer*; the dislocation cell structure can be revealed by

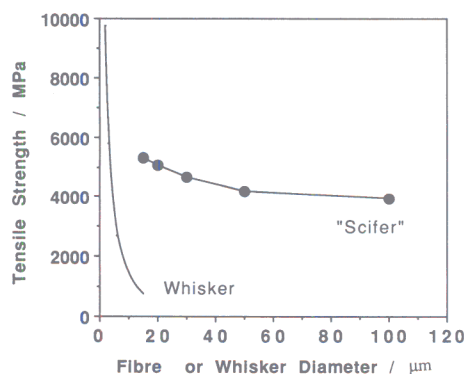


Fig. 1. Tensile strength as a function of sample diameter, for single crystal whiskers of iron [1] and for *Scifer* [2]. Note that the strength of *Scifer* is much less sensitive to size.

the fact that the distribution of strain energy in the proximity of a low misorientation boundary leads to preferential evaporation of material, and, hence, contrast in the image [3].

## 2. Experimental

### 2.1. Material and heat treatment

The average chemistry of the steel involved is quite simple, Fe–0.2wt%C–1.2wt%Si–

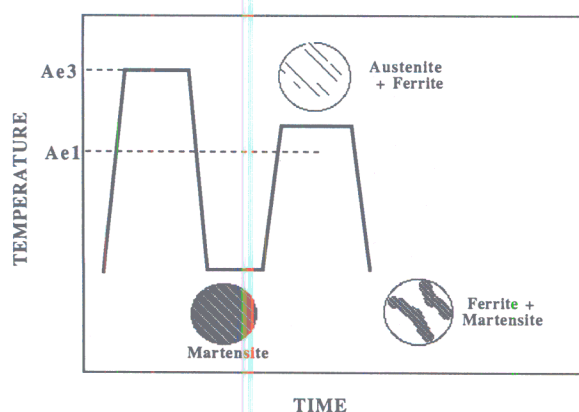


Fig. 2. Schematic illustration of the heat-treatment used in the production of Scifer, and of the resultant starting microstructure. Under equilibrium conditions, the steel becomes fully austenitic at temperatures above the  $Ae_3$  temperature. Within the temperature range  $Ae_1$ – $Ae_3$  it is an equilibrium mixture of ferrite and austenite, the proportion of austenite decreasing to zero as the temperature tends towards  $Ae_1$ .

1.5wt%Mn. The purity has to be consistent with the fact that the final fibre diameter is sometimes expected to be less than 10  $\mu\text{m}$ . The inclusion content must therefore be kept at a minimum. The carbon concentration is much smaller than in pearlitic wires, and the silicon concentration is somewhat larger. Although the wire is drawn as for conventional piano wire, the heat-treatment is radically different from that involved in the patenting process (fig. 2).

Rods of diameter 10 mm are first quenched to martensite, and then intercritically annealed in the  $(\alpha + \gamma)$  phase field. This induces the growth of a small quantity of austenite in the form of layers between the packets of the original martensite. The latter tempers during the intercritical anneal, and on quenching to ambient temperature, the layers of austenite soon decompose into regions of high-carbon martensite containing some retained austenite. The light areas in fig. 2 are the regions of martensite which are tempered during the intercritical anneal; they probably do not contain any carbides, since the carbon is expected to migrate into the newly formed austenite.

Transmission electron microscopy [4] suggests that the microstructure of the drawn fibre in its

final condition consists of a dislocation cell structure which is slightly elongated along the drawing direction. The cell size along the wire diameter is not known and their size is generally unclear from the transmission micrographs. A typical dislocation cell structure would contain dislocations localised at the cell walls, and relatively clean cell interiors. It has not yet been possible to distinguish clearly the martensitic and tempered martensitic regions in the drawn wire microstructures.

## 2.2. The instrument and sample preparation

A VSW Technologies APFIM 200 atom-probe/field ion microscope equipped with a reflectron time-of-flight mass spectrometer was used in the experiments. The pulse fraction and pulse rate used for field evaporation were 20% and 200 Hz, respectively. Although the instrument is capable of detecting up to eight ions per pulse, the conditions were adjusted such that there were never more than three, and in the vast majority of cases only one, ion recorded per pulse.

The data in table 1 represent a total of 117 000 ions collected during the field evaporation of ferrite, and they confirm that the definition of the range file is satisfactory. Note that the discrepancy between the ferrite carbon concentration and the bulk carbon concentration is because of the presence of minute carbon rich regions, as discussed later in the paper.

Scifer comes in the form of a woven seven-strand wire, each fibre being about 7  $\mu\text{m}$  in diameter. After untangling, individual fibres were mounted into copper tubes. The free end of each

Table 1

Comparison of time-of-flight mass spectrometer data from some 117 000 ion with the bulk chemistry of Scifer; note that the mass spectrometer data refer only to elements in solid solution in the ferrite

	TOF data (at%)	TOF data (wt%)	Bulk chemistry (wt%)
C	$0.50 \pm 0.02$	0.11	0.20
Mn	$1.41 \pm 0.03$	1.41	1.5
Si	$2.60 \pm 0.05$	1.33	1.2

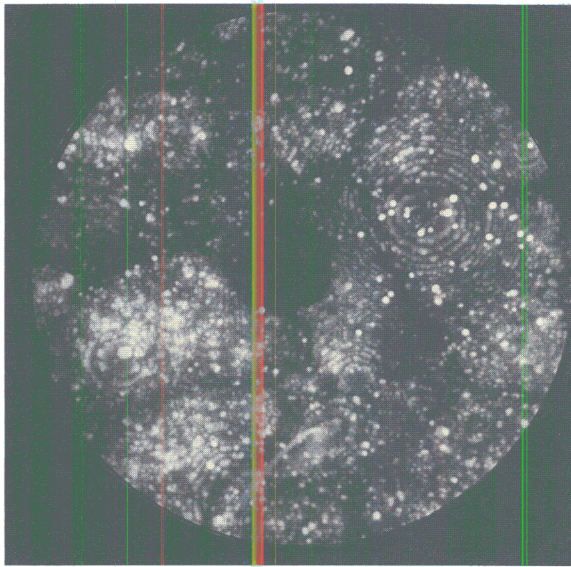


Fig. 3. Field ion images of as-received Scifer, using neon as the imaging gas and with a sample temperature of 22 K. The dark bands represent the dislocation cell structure.

fibre was then coated with a bead of insulant ("lacomit"). The sample was then dipped into a 2% perchloric acid in butoxyethanol solution for electropolishing at 20 V until the insulated end dropped off. This single state technique gave excellent tip shapes and dimensions for field ion microscopy.

### 3. Dislocation structure

Fig. 3 shows a representative FIM image of as-received Scifer in the cold drawn condition. The ultrafine dislocation cell structure is clearly revealed, the cell size in a direction normal to the drawing direction being approximately 10–15 nm. The small crystallographic misorientations across some of the cell boundaries are apparent in the approximate continuity of the rings of imaged atoms across the cell walls. The fact that this continuity is not obvious across all the cell walls might indicate larger misorientations caused by the severe deformation.

#### 3.1. The strength of scifer

The problem of general yield is rather different from a Hall–Petch relationship as the grain size reduces to below about 1  $\mu\text{m}$ , because it is no longer the initiation of sources in an adjacent grain that determines yield. Instead, it is the stress to operate a source within a grain that is the critical event in triggering macroscopic yielding.

Langford and Cohen [5,6] have treated the problem of strengthening due to the fine cell structures formed in drawn wires. They considered the energy required to spread and expand dislocation loops across the glide planes of the cells, during the deformation of the cells along their long directions. The strength  $\sigma$  was found to depend on the inverse of the cell size:

$$\sigma \approx \sigma_0 + 2.5Gb(\bar{d})^{-1}, \quad (1)$$

where  $\bar{d} \approx 10\text{--}15$  nm is the cell size normal to the drawing direction,  $b \approx 0.25$  nm is the magnitude of the Burgers vector of the slip dislocations,  $G \approx 80$  GPa, and  $\sigma_0$  is the friction stress. Thus, the strengthening due to the cell size (i.e.  $\sigma_{\text{Cell}}$ ) can easily be calculated to be approximately 5000–3300 MPa (for  $\bar{d} \approx 5\text{--}15$  nm). The cell structure clearly is the major contribution to the total strength of the wire. The term  $\sigma_0$  can be factorised as follows:

$$\sigma_0 = \sigma_{\text{Fe}} + \sum_i \sigma_i, \quad (2)$$

where  $\sigma_{\text{Fe}}$  is the strength of pure annealed iron at ambient temperature, and  $\sigma_i$  are the contribu-

Table 2  
Contributions to the strength of Scifer at ambient temperature, in MPa

	$\sigma$ (MPa)
$\sigma_{\text{Fe}}$	217
$\sigma_{\text{Mn}}$	63
$\sigma_{\text{Si}}$	83
$\sigma_{\text{C}}$	800
$\sigma_{\text{Cell}}$	3300–5000
Total (dissolved C)	4463–6163
Total (precipitated C)	3663–5363



tions from solid solution strengthening. Using published data [7–9], it is possible to arrive at the strength contributions listed in table 2. Thus the total yield strength is estimated to be about 4.5–6.1 GPa, if all the carbon is assumed to be in solid solution, and 3.7–5.3 GPa, if the carbon is precipitated and therefore assumed to contribute little to the overall strength. Clearly, the sum of the contributions listed in table 2 compares rather well with the available data on the tensile strength of Scifer at 4–5.3 GPa [2,4].

### 3.2. The role of carbon

The function of carbon in Scifer is interesting and requires some further investigation and comment. The intercritical annealing heat-treatment (followed by quenching to ambient temperature) should give a microstructure of high carbon martensite ( $C > 0.2$  wt%), its associated small quantity of retained austenite, and ferrite. There is also the possibility of some minute cementite

particles due to any autotempering of the martensite, although transmission electron microscopy has not revealed it. This is the microstructure before any deformation.

Atom-probe experiments have been carried out to understand better the distribution of carbon in the high strength steel wire after the severe drawing deformation. Time-of-flight mass spectroscopy can easily reveal the concentration in solid solution. Fig. 4 shows data obtained during depth profiling as the as-received sample was field evaporated. The data were collected on an atom by atom basis, but to visualise the concentration, they are presented as the concentrations of carbon in each successive block of 1000 atoms. Given that the presence of a cementite particle would lead to a carbon concentration of around 25 at%, it is clear that the carbon is in solid solution, even though it is not completely homogeneously distributed (fig. 4). The average carbon concentration estimated from a dataset of some 117 000 ions collected was found to be  $0.5 \pm 0.02$

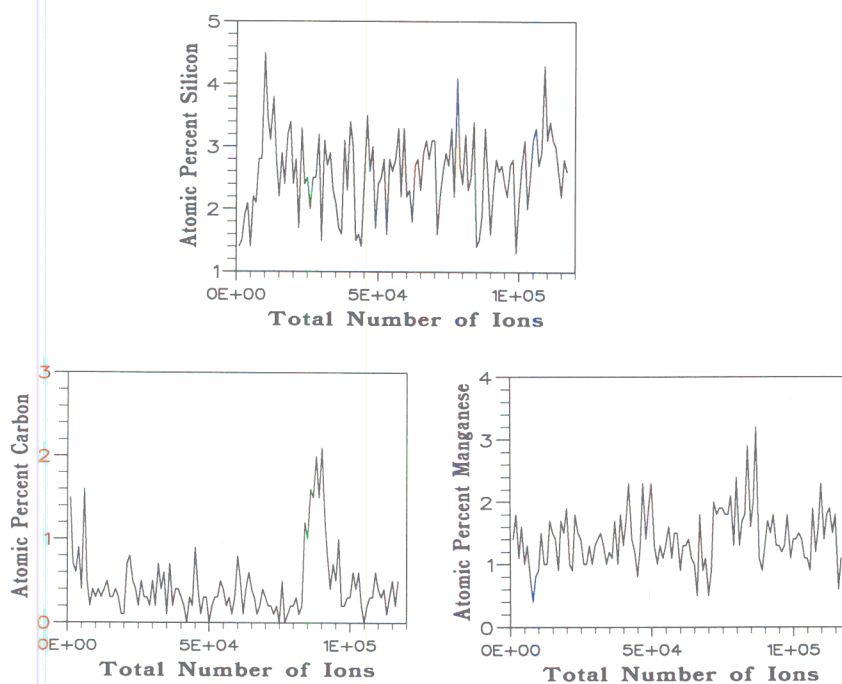


Fig. 4. Carbon, silicon and manganese concentrations of the ferrite in as-received Scifer wire. Averaged over each successive 1000 ion block.

at% (i.e. 0.11 wt%). Thus, a great excess of carbon is present in solid solution in the ferrite, amounting to about half the total carbon concentration of the alloy (0.2 wt%). Further work is needed to check whether the inhomogeneous distribution of carbon (within the range 0.1–2 at%) correlates with any structure feature. The other elements are essentially homogeneously distributed in the ferrite.

The cell walls did not show any significant degree of carbon segregation. However, on occasions, very large but extremely narrow carbon spikes were seen, as illustrated in fig. 5, while probing into a cell boundary. It could be that this indicates the presence of extremely small carbides (100 atoms at most), although the carbon concentration is far too high for any of the common iron carbides. It could be speculated that they represent regions of graphite since the steel has a large silicon concentration which favours the precipitation of graphite over that of cementite. If they are carbides, they must have formed at a relatively low temperature since there is no obvious difference in the silicon or manganese concentrations within the carbon-rich regions when compared with the surrounding matrix ferrite. Note that the actual carbon concentration in the carbide is uncertain since the choice of a smaller block size would yield a larger concentration.

An additional experiment was conducted by annealing the deformed wire at 400°C for 90 min. Field ion images confirmed that this had no observable effect on the dislocation structure, al-

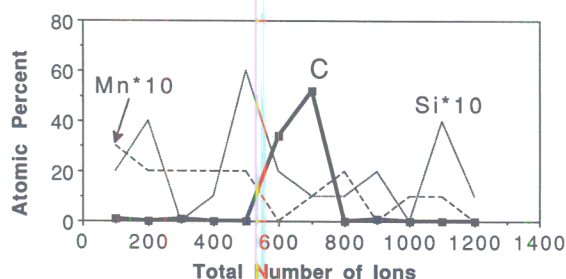


Fig. 5. Concentration profiles observed during atom probing along a cell wall. The silicon and manganese concentrations are multiplied by a factor of ten.

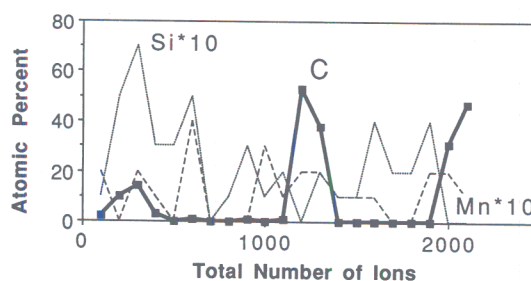


Fig. 6. Concentration profiles during atom-probing along cell boundaries in a sample annealed at 400°C for 90 min. The silicon and manganese concentrations are multiplied by a factor of ten.

though the appearance of several relatively broad carbon spikes during depth profiling indicated that the annealing treatment was inducing the precipitation of some very fine carbon-rich regions (fig. 6).

The starting microstructure prior to deformation contained regions of martensite formed during intercritical annealing, which are expected to contain carbon concentrations far in excess of the average level of 0.2 wt%. Instead, the results show that there is a relatively uniform carbon concentration in the matrix at a concentration of about 0.11 wt%. It can be tentatively concluded that the remaining carbides are present as very fine particles which have precipitated after the deformation process (since the silicon concentration in particular does not seem to be different in the carbon rich regions). The results confirm directly that there is a large excess of carbon trapped in solid solution in the ferrite. It appears that the extreme degree of deformation required to produce the fibre has led to a *mechanical homogenisation* of the starting microstructure.

It is interesting to note that similar mechanical homogenisation effects have been reported when mixed microstructures of ferrite and cementite are heavily deformed. Whilst the solubility of carbon in ferrite which is in equilibrium with cementite is very small indeed, large deformations are well known to force the dissolution of cementite, at temperatures below that at which austenite might form first. This is commonly assumed to happen in the region of intense defor-

mation during the ballistic penetration of steel. The formation of the so-called "white layers" on pearlitic rail steels subjected to severe deformation is another example of this phenomenon. The white layers are believed to form without any growth of austenite, but the carbon nevertheless enters solid solution in the ferrite [10]. There are two mechanisms known to induce carbide dissolution in metastable microstructures. Firstly, the deformation causes a fragmentation of the cementite to a size well below its critical nucleus size, so that the cementite dissolves. Secondly, the stability of precipitates is known to be affected by the presence of dislocations, where the carbon may segregate to dislocations in preference to precipitation [11,12].

#### 4. Conclusions

It appears that much of the strength of the 5 GPa steel wire has its origins in the ultrafine dislocation cell structure produced as the wire is drawn down to a few micron diameter fibre from a starting size of 10 mm. An interesting observation is that the deformation process has forced most of the carbon into solid solution. There is some evidence for very fine regions with extremely large carbon concentrations, but more work is necessary to discover their origin and structure.

#### Acknowledgements

The authors are grateful to Professor C. Humphreys for the provision of laboratory facilities, and to Dr. T. Inoue and his colleagues at Kobe Steel, for introducing us to *Scifer*, and for providing several micrographs and other data. The work presented here was carried out under the auspices of the "Atomic Arrangements: Design and Control" project, which is a collaborative venture between the University of Cambridge and the Japan Research and Development Corporation. We would also like to express our heartfelt thanks to Bob Waugh and Carl Richardson for the APFIM200 and for all kinds of help.

#### References

- [1] S.S. Brenner, *J. Appl. Phys.* 27 (1956) 1484.
- [2] Anonymous, *Kobelco Technology Review* No. 8 (Kobe Steel, Ltd., Japan, 1990).
- [3] D.G. Brandon, B. Ralph, S. Ranganathan and M.S. Wald, *Acta Met.* 12 (1964) 813.
- [4] T. Inoue (Kobe Steel), Private communication to H.K.D.H. Bhadeshia, 1991.
- [5] G. Langford and M. Cohen, *Trans. Am. Soc. Met.* 62 (1969) 623.
- [6] G. Langford and M. Cohen, *Met. Trans.* 1 (1970) 1478.
- [7] T.L. Altshuler and J.W. Christian, *Proc. R. Soc. London A* 261 (1967) 253.
- [8] W.C. Leslie, *Met. Trans.* 3 (1972) 5.
- [9] G.R. Speich and H. Warlimont, *J. Iron Steel Inst. (London)* 206 (1968) 385.
- [10] S.B. Newcomb and W.M. Stobbs, *Mater. Sci. Eng.* 66 (1984) 195.
- [11] D. Kalish and M. Cohen, *Mater. Sci. Eng.* 6 (1970) 156.
- [12] H.K.D.H. Bhadeshia, *Acta Met.* 28 (1980) 1103.